Penerbit Akademia Baru

Journal of Advanced Research in Fluid Mechanics and Thermal Sciences

Journal homepage: www.akademiabaru.com/arfmts.html
ISSN: 2289-7879

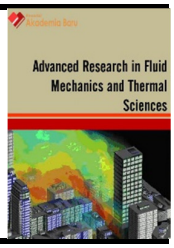

The Effects of CO_2 Variation on Hydrodynamic and Thermal Diffusive Stability of Biogas–Air Flame

Open Access

Mohd Suardi Suhaimi[1,*], Aminuddin Saat[2], Mazlan Abdul Wahid[2], Mohd Fairus Mohd Yasin[2]

[1] Department of Chemical Engineering, Faculty of Chemical & Energy Engineering, Universiti Teknologi Malaysia, 81310 Skudai, Johor, Malaysia
[2] Department of Thermofluids, Faculty of Mechanical Engineering, Universiti Teknologi Malaysia, 81310 Skudai, Johor, Malaysia

ARTICLE INFO

Article history:
Received 29 October 2018
Received in revised form 1 December 2018
Accepted 9 December 2018
Available online 12 December 2018

ABSTRACT

Understanding the effects of CO_2 on biogas combustion is vital as it occurs naturally as one of the major biogas content aside from CH_4. In the present study, burning rate and flame stability of simulated biogas combustion have been investigated at 1 atm and 298K. CO_2 dilution was set at 20, 40 and 50% to emulate typical biogas content. Experiment was performed using spherically expanding flame to include the effect of stretch on flame propagation. Results from experiment were compared with numerical results as well as data and correlations from literature. Results reveals a linear trend between CO_2 dilution and burning rate reduction. Compared to pure CH_4, peak burning rate steadily decreases to 21.17%, 34.14% and 45.15% as CO_2 dilution was increased from 20 to, 40 and 50% respectively. Chemically, CO_2 could slow down the reactions that produces OH and CO radicals important for CH_4 dissociation. Physically, CO_2 could modify mass and thermal diffusion pattern as indicated by the Markstein length that shows noticeable changes as CO_2 was increased. In terms of stability, CO_2 tends to stabilize flame by suppressing the thermal-diffusive and hydrodynamic instability.

Keywords:
Biogas, spherically expanding flame, burning rate, Markstein length, thermal-diffusive instability, and hydrodynamic instability

1. Introduction

Depletion of fossil fuel has attracted studies on renewable alternative fuels. With current rate of consumption, it is expected that fossil fuel such as oil and natural gas could be completely consumed by 2042 [1]. Biogas has been regarded as one of the promising fuel to serve as an alternative to the depleting fossil fuel as it is renewable. Depending on its sources, biogas mainly contains approximately 50-70% methane, 30-50% carbon dioxide and trace gases at smaller quantity. It can be produced by anaerobic fermentation of municipal to agricultural waste using microorganisms called methanogens. Using biogas can also help in reducing Green House Gas

* *Corresponding author.*
E-mail address: mka2global@gmail.com (Mohd Suardi Suhaimi)

emission since its combustion generates less pollutants compared fossil fuels [2]. Many studies are directed towards enhancing biogas production and processing. These includes the screening for potent methanogens, optimized process and enrichment [3]. Nevertheless, fundamental studies on biogas combustion characteristics are relatively scarce. The presence of CO_2 in biogas at varying amount could alter combustion characteristics to the point that it could become unpredictable thus may complicate the commercial use of biogas [4]. It may cause reduction in flame speed and flammability limits due to reduced heat release and flame temperature [5]. Changes in mass and heat diffusivity due to the presence of CO_2 may further contribute to uncertainty in biogas combustion [6]. The effect of radiation on the other hand is negligible for CO_2 diluted methane-O_2 mixture [7].

Laminar burning rate is among the fundamental combustion characteristics that is used to describe the laminar premixed combustion of certain fuels [8]. Accurate measurement of laminar burning rate permits the understanding of propagation rates, heat release, quenching and emission characteristics. It could be derived from data of flame speed that serves as the primary data. There are several methods to determine flame speed such as flat flame [9 & 10], counterflow flame [11 & 12] and spherically expanding flame [13-16]. The latter constitutes the most versatile and accurate method to date [17]. The stretched and unstretched laminar flame speed and burning rate of spherically expanding flame can be obtained from schlieren photographs as described by Gillespie et al. [18].

Markstein length, flame thickness and density ratio are another important flame characteristics. Markstein length describes the effect of stretch on flame propagation and is related to thermal-diffusion instability while flame thickness and density ratio are related to hydrodynamic instability [19]. Determination of these parameters could help to gauge whether certain fuel mixture could combust in a stable and safe manner under certain conditions.

Previous studies on biogas burning rate are limited to biogas with methane content of more than 60% often termed as high quality biogas [20]. A study by Walsh et al. shows obvious reduction in burning velocity by more than 50% as CO_2 was varied from 20% to 40% within the equivalence ratio range of 0.6 to 1.4. Qin et al varied CO_2 to up to 45% and observed a noticeably higher burning rate compared to Walsh et al within narrower equivalence ratio range of 0.6 to 0.75. Park et al extended data by Qin et al through a numerical study that covers wider equivalence ratio from 0.6 to 1.4 with maximum CO_2 content of 45%. Their data fit well with Qin et al within the equivalence range of 0.6 to 0.75. So far, only a recent study by Nonaka and Pereira [21] investigated low quality biogas using heat flux method with unity Lewis number as a constraint. The presence of CO_2 in biogas has been shown to increase Lewis number making flames stretch amenable to thermo-diffusive instability [22]. Also, the assumption of unity Lewis number is only valid for adiabatic flames. The presence of CO_2 may give rise to changes in diffusion pattern as well as kinetics which are affected by stretch [23 & 24]. Diffusion has been known to affect kinetics of combustion and thus should not be neglected [25]. Data on biogas flame behavior in terms of diffusional-thermal and hydrodynamic instabilities are also still lacking in literature. The former is indicated by Markstein length while the latter by density ratio and flame thickness.

Studying biogas combustion characteristics at wider range of CO_2 (up to 50%) could help in understanding the effects of CO_2 variation on the combustion of biogas which typically contains large percentage of CO_2. It could also justify if unrefined low quality biogas could be directly used in commercial combustors as the cost of enriching biogas is quite high [26 & 27]. Moreover, experimental studies on biogas up to 50% CO_2 has never been reported in literature. A numerical study by Fischer and Jiang [28] reported that at this particular CO_2 percentage, biogas combustion would depend on direct decomposition of methane instead of hydrogen atom abstraction. This

claim however has never been substantiated by experiments. The objective of this study is to investigate the effect CO_2 on the burning rate and the flame stability of simulated biogas-air mixture at 1 bar and 298K using spherically expanding flame method coupled with Schlieren photography. The CO_2 contents biogas-air mixtures were set at 20%, 40% and 50% to represent biogas with different quality from low to high, and thereafter labeled as BG50, BG60 and BG80 respectively. Schlieren photography enables the detection of density gradient resulting from combustion. It also permits the exclusion cellular flames that render the smooth flame front assumption void.

2. Methodology

Figure 1 shows the experimental setup consisting of a cylindrical constant volume combustion chamber (CVCC) with a volume of 29.3L with two 190mm quartz optical windows and a linear schlieren photography setup. The CVCC is connected to ignition box that supply ignition energy at the center of the CVCC through a pair of electrodes. The ignition energy was set at 25mJ. The linear schlieren photography setup is made up of collimating and focusing lens, a Phantom 7.1 high-speed camera, and an LED light source. Using partial pressure filling technique, the CVCC was filled with methane, CO_2 and air with different partial pressure that correspond to the desired equivalence ratio ranging from 0.5 to 1.2 after it has been vacuumed. CO_2 content was varied from 20% to 50% while the initial pressure for each experiment was set at atmospheric pressure with initial temperature of 298K. Ignition was controlled using a desktop computer with a LabView 7.1 software connected to the ignition box after the capacitor was charged.

The developing flame videos were recorded at 2000 frames per second with the Phantom 7.1 high speed camera. The recorded cine videos were then converted to image files for further analysis using image processing softwares. Adobe Photoshop CC software was used to convert to the images of the spherical flames to binary images. These binary images were then analyzed using a Matlab script file to obtain flame area and the radii. The obtained radii were then tabulated in a spreadsheet file where the flame speed was obtained by differentiating with respect to time a first order fit of five points.

For spherically propagating flames, two different stretch phenomena should be considered. The first one is the tangential strain rate (a_{tt}) acting on the flame surface while the second arises from flame curvature. The latter could also be described as the product of local curvature (h) arithmetic mean and local propagation velocity relative to reactant fluid (S_b). S_b can be viewed as flame curvature relative to the origin where the ignition starts. Therefore, in terms of h and S_b, flame stretch α could be expressed as:

$$\alpha = a_{tt} + 2S_b h \tag{1}$$

For spherical flames, the flame speed and flame stretch are represented by the following expressions;

$$S_n = \frac{dr}{dt} \tag{2}$$

$$\alpha = \left(\frac{2}{r}\right)\frac{dr}{dt} \tag{3}$$

$$\alpha = \left(\frac{2}{r}\right)S_n \tag{4}$$

Including the effect of stretch on flame speed gives:

$$S_s - S_n = L_b \alpha \quad (5)$$

Where S_s is the unstretched flame speed and L_b is the proportionality constant Markstein length. Markstein length represents the effect of stretch rate (α) on stretched flame speed S_n and it is given by the slope of flame speed against stretch plot. Extrapolation of the plot to a point of zero stretch gives the unstretched flame speed that is used in the determination of burning rate, u_L, by the relation:

$$u_L = S_s \frac{\rho_b}{\rho_u} \quad (6)$$

The term $\left(\frac{\rho_b}{\rho_u}\right)$ represents the density ratio of the burned and unburned gas of constant pressure combustion under adiabatic condition. Burning rate is essentially the velocity of the cold reactants normal to the reaction zone plane [18].

Flame thickness is calculated by the following expression [29, 30]:

$$\delta_l = \frac{\lambda}{C_p \rho_u u_L} \quad (7)$$

where λ and c_p are the unburned gas thermal conductivity and specific heat respectively. λ, ρu, ρb and c_p are determined using the Gaseq Chemical Equilibrium software

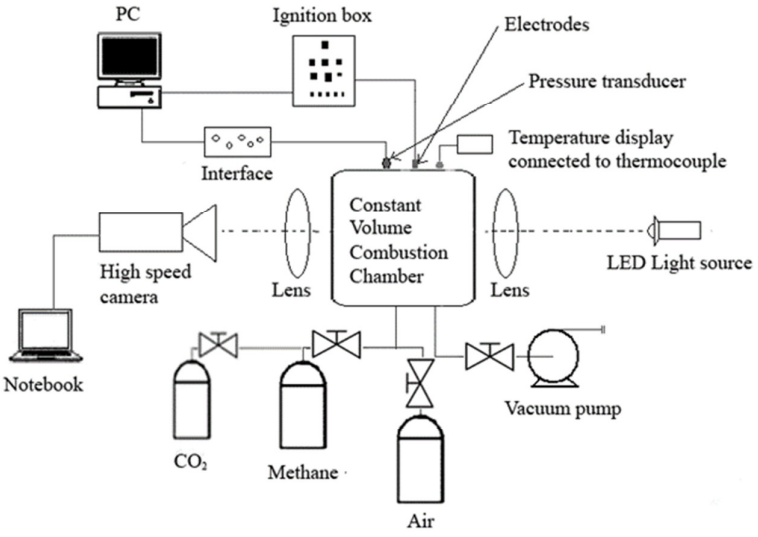

Fig. 1. Experimental Setup.

3. Results

3.1 Biogas flame speed and burning rate

The images of spherical flame at a radius of approximately 40 mm for different equivalence ratio of each fuels are shown in Figure 2. The flames for each equivalence ratio and CO_2 percentage are quite stable with no observable cellularity that could arise from thermal-diffusive instability. Cellularity has also been reported for biogas air mixtures at elevated pressures [31]. Hydrodynamic

instability and buoyancy were also not observed in this study. CO_2 could have a stabilizing effect under atmospheric condition.

Figure 3 shows the comparison of flame propagation speed for pure CH_4 and each biogas for the equivalence ratio of 0.9. During the first ten millisecond after ignition, the flame speed of all flames exhibit typical reduction caused by diminishing radicals from the supplied electrical spark. This region often described as the spark affected region. The flame then started to stabilize to reach a steady flame speed towards the end of combustion. Thus, in terms of trend, the flame speed of each fuel are almost identical. However, in terms of magnitude, the difference in flame speed between pure CH_4 and each biogas are quite significant. There is about 23% reduction in flame speed for every 20% CO_2 percentage increment i.e. between pure CH_4, BG80, BG60 and BG50. This suggest the strong influence of CO_2 in reducing the flame speed. CO_2 may have influence both the diffusion and kinetics of combustion resulting in the observed proportional reduction in flame speed as CO_2 level increases [32].

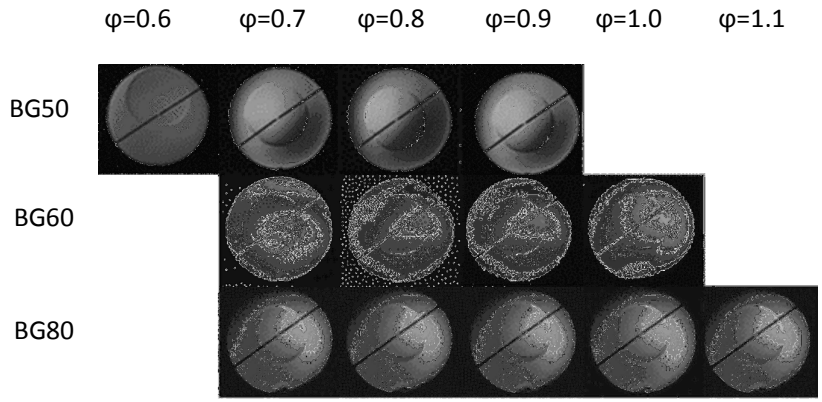

Fig. 2. Flame image of each biogas mixture at radius of 40mm.

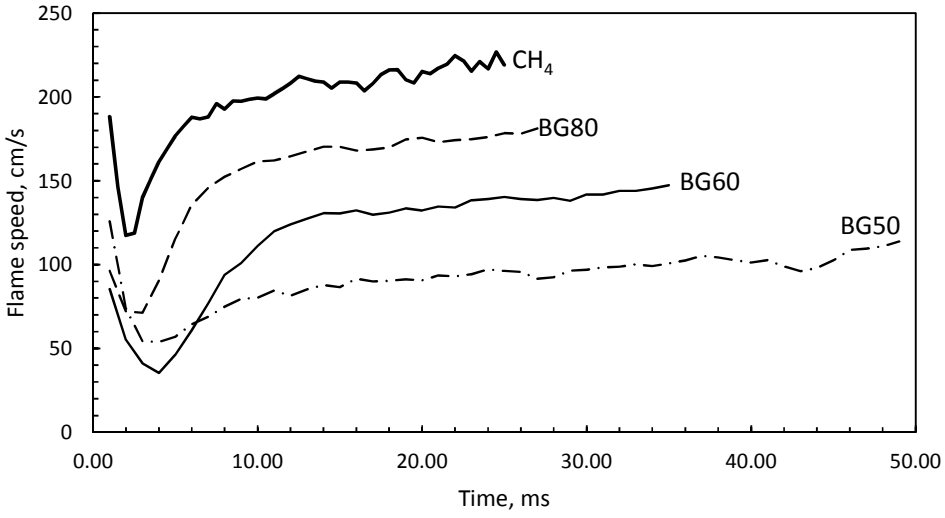

Fig. 3. Comparison of flame speed variation with time for each biogas at equivalence ratio of 0.9.

Figure 4 shows the variation of burning rate of pure CH_4, and all of the simulated biogas-air mixtures over a wide range of equivalence ratios determined by using Equation 6. Data from the early stage of combustion were omitted as these data are mostly affected by the energy from the ignition spark and could lead to over or underestimation of unstretched flame speed [33]. Only data within the quasisteady region are considered in the determination of unstretched flame speed and Markstein length as data beyond this region are either affected by ignition energy or confinement effect [33].

The burning rates for all the mixtures share the quadratic trend with equivalence ratio. There are however obvious differences in burning rate magnitude and the corresponding equivalence ratio at which the peak of the burning rate occur between all of the simulated biogas and pure CH_4. The maximum burning rate tend to decrease with an increase in CO_2 percentage and it also occurs at leaner equivalence ratio. For BG80, the maximum burning rate occurs at equivalence ratio of 1.0 with a magnitude of 29.68cm/s, approximately 21.4% lower than pure CH_4 (37.75 cm/s at equivalence ratio of 1.1). The reduction continues at CO_2 percentage of 40% and 50% where the burning rate decrease to 24.84 cm/s and 21.68 cm/s respectively.

The shift in the peak of burning rate to the leaner mixtures could also be observed in Figure 4. A study by Hinton and Stone [31] also showed the shift in peak burning rate away from stoichiometric as CO_2 increases. Such shifting phenomenon in peak burning rate was not observed by other studies in literature. Hinton and Stone attributed this phenomenon to Le Chatelier principle where the presence of CO_2 could change the equilibrium of biogas burning as CO_2 is one of the products of combustion. As stated by Le Chatelier principle, a change in the concentration of reactants or products (aside from temperature and volume) will cause any particular reaction to counteract the effect of the change.

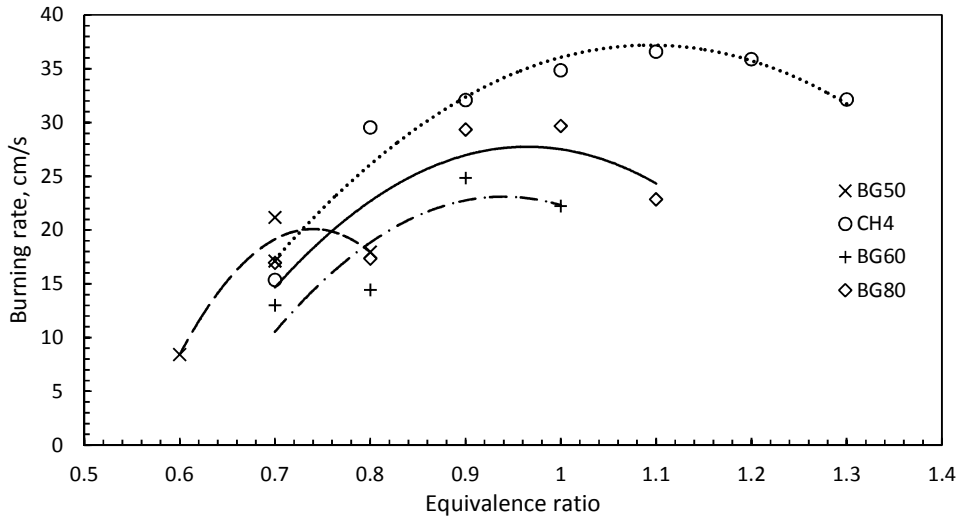

Fig. 4. Comparison of burning rates variation with equivalence ratio between pure CH_4 and each biogas.

The value of peak burning rate however, are in good agreement with burning rate data from literature as shown in Figure 5. The peak burning rate also reduces appreciably and it shifts to leaner side as CO_2 increases marking the significance of CO_2 effect. This could be attributed to the method used where in the case of spherical flame, the burning rate of a positively curved flame could be enhanced provided that the mass transfer into the flame zone is larger than the heat

transfer out from the flame zone [24]. Such phenomenon will not be observed in other method such as by Nonaka and Pereira [21] since the Lewis number was constrained to 1 implying balance between mass and thermal diffusion thus excluding the effect of stretch on flame propagation. Coupling between kinetic and diffusion may also be another contributing factor to this observation.

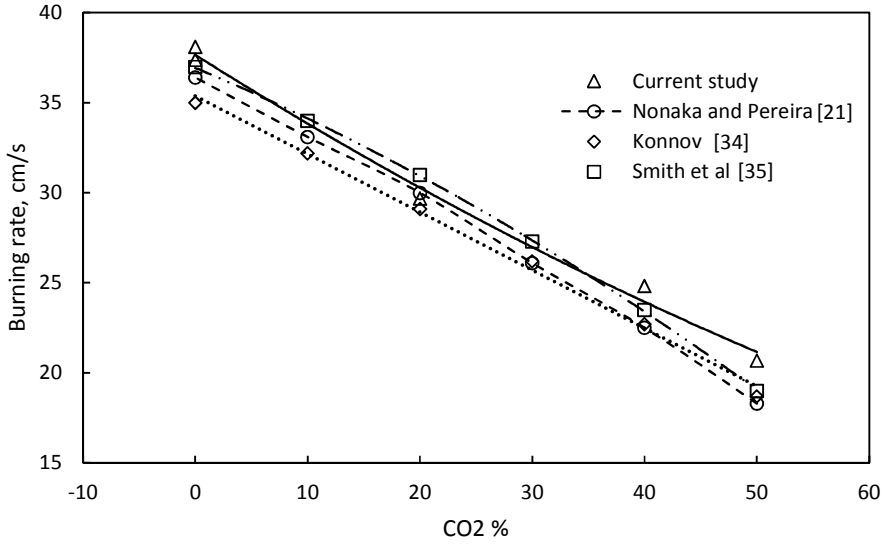

Fig. 5. Effects of $C0_2$ percentage on maximum burning rate for pure CH_4 and each biogas mixture.

Also, the lean limit of BG50 extend to 0.6, 0.1 lower than pure CH_4, BG80 and BG60. This could be due a change in kinetics at this particular condition that enables the mixture to ignite. Certain reaction has been shown to become more significant at atmospheric condition with 50% CO_2 such as H+ CO_2 ⇌ OH + CO which is a chain branching reaction. This reaction would play a greater role in biogas combustion especially under leaner condition [28]. It is likely that the rate constant for this reaction is enhanced by an increase in pre-exponential factor of the Arrhenius expression rather than the activation energy as temperature is kept constant in this study. Soret diffusion could also aid the ignition of light hydrocarbon fuels. It has been shown to enhance spherical flame ignition and propagation by modifying local equivalence ratio [36]. Due to the effect of Soret diffusion, the local equivalence ratio of BG50 could actually be slightly higher than 0.6 enabling it to combust.

The reduction of burning rate is a direct effect of CO_2 as it increases from 20%, 40% and 50%. CO_2 could thermally and chemically affect biogas combustion. Physically, CO_2 could absorb some of the heat released during combustion reducing flame temperature and thus the burning rate. This is also termed as the dilution effect. This is demonstrated in Figure 6 that shows the adiabatic flame temperature that steadily decreases with CO_2 percentage. CO_2 has been known as one of the greenhouse gasses that could absorb heat due to its relatively large heat capacity. Figure 5 shows the variation of maximum burning rate with CO_2 content. As discussed earlier, CO_2 may reduce the burning via physical or dilution effect or modification in the kinetic of combustion. From the graph, the trend in burning rate reduction from 0% (representing pure methane) to 50% CO_2 can be approximated by a linear trend that agrees well with the trend reported in literature.

Chemically, CO_2 could alter the kinetic of combustion by reduction in certain species or radicals that are important in sustaining combustion. It is likely that the presence of CO_2 may alter several rate constants of important reactions by increasing the frequency factor of the Arrhenius

expression. Frequency factor is related to the number of collision during reaction and also the portion of collision that is in correct geometry for reaction to proceed. One of the most important radicals is OH radicals that are produced after ignition and help to sustain combustion via chain branching. Through chain branching, OH radical continuously abstract H atom from CH_4 leading to CH_4 decomposition and consequently releasing heat. The rate at which OH radicals produced is significantly affected by CO_2 [4]. When present at 50% or more, significant change in kinetics would occur especially for leaner mixture [4]. As the equivalence ratio increases (and also CO_2), direct decomposition of CH_4 through the reaction $CH_4+M(CO_2) \rightleftharpoons CH_3+H+M(CO_2)$ will play a much more important role in ignition and combustion [28]. Direct decomposition of CH_4 produces CH_3 and H radicals in contrast to OH and CH_3O radicals. Moreover, as CH_3 increases, the likelihood this radicals to recombine also increases via the chain termination reaction $2CH_3+ M(CO_2) \rightleftharpoons C_2H_6 + M$, contributing to the inhibition of combustion to the point where the rich limit is attained.

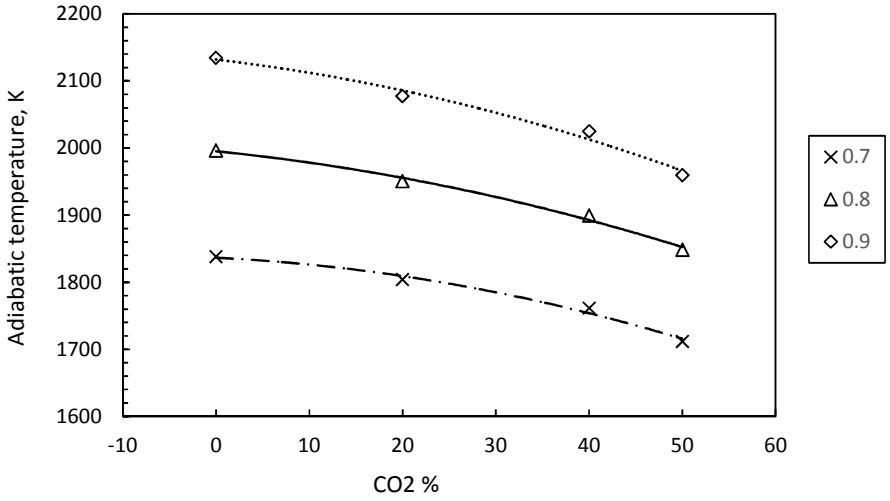

Fig. 6. Variation of adiabatic temperature with CO_2 content for flame at equivalence ratio of 0.7, 0.8 and 0.9.

3.2 Biogas Markstein length, flame thickness and density ratio

Markstein length is a parameter that indicates the effect of stretch on flame. It also indicates the propensity of flame to become stable or unstable towards mass-thermal diffusion imbalance. Larger magnitude of Markstein length indicates greater effect of stretch on flame resulting in better stability and vice versa. For a spherically expanding flame, stretch is contributed by both flame curvature and aerodynamic strain. Figure 7 shows the comparison in the magnitude of Markstein length between pure methane, BG50, BG60 and BG80. The data of pure CH_4 Markstein length is from the previous work by Suhaimi et al. [37]. The overall trend of Markstein length variation with equivalence ratio is almost identical between pure methane and the simulated biogas where it increases with equivalence ratio. Positive values of Markstein length suggest the stabilizing effect of CO_2 on biogas flame across the equivalence ratio.

There are however differences in the degree at which the Markstein length increases with CO_2 content. At higher CO_2 content especially for BG50, the increase in Markstein length tend to be sharper as the equivalence ratio increases. This suggests a more significant role of stretch as CO_2 increase. This trend continues as equivalence increase to 0.9 where the Markstein length of both

BG50 and BG60 deviate further from that of pure methane and BG80. Apparently the presence of CO_2 could significantly enhance the effect of stretch on flame propagation. Stretch may also assist mixture ignition and flame initiation especially for mixture with smaller Lewis number [36].

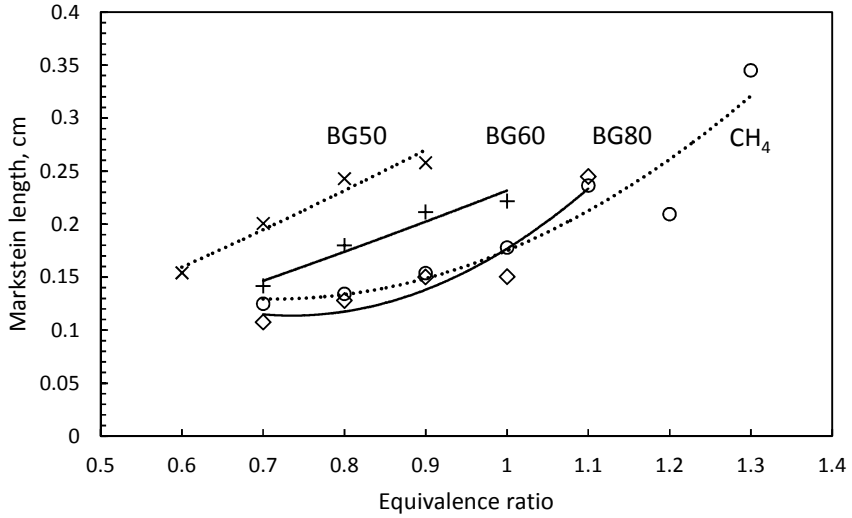

Fig. 7. Comparison of Markstein length variation with equivalence ratio of CH_4 and each biogas.

Also, buoyancy was not observed for all flames even for leanest mixture. Normally, weak flames are more susceptible to buoyancy that could also affect flame morphology [31]. It could also lead to a form of instability commonly termed as the Rayleigh-Taylor instability. In the case of spherically expanding flame, the fragment of the flame that propagates downward could be subjected to this kind of instability. Cellularity could also occur if the thickness of the flame is sufficiently low [31]. In this study however, no cellularity was observed for all of the mixtures indicating that the thickness is sufficiently high to inhibit cellularity.

Increase in Markstein length also indicates a change in mass-thermal diffusion. Diffusion is a transport process that is driven by difference in concentration (Fickian), molecular weight (preferential) or temperature (Soret) [37]. Due to the presence of CO_2 that has different molecular weight and heat capacity, modification on the aforesaid types of diffusion could be expected. Compared to CH_4, CO_2 has higher molecular weight and heat capacity, thus when present especially at sufficiently high amount, could alter the concentration and temperature gradient, as well as diffusion of CH_4 and O_2 into the reaction zone.

Another type of instability is hydrodynamic instability which is influenced by thermal expansion at the flame front. Flame thickness and density ratio (ρ_u/ρ_b) are two parameters that influence hydrodynamic instability at the flame front where the former has an inhibiting effects while the latter has promoting effects [36]. In contrast to flame stretch that affect flame structure, hydrodynamic instability influence flame geometry [38]. For outwardly propagating spherical flames, it becomes more significant at larger flame radii as opposed to flame stretch that is more significant during the earlier stage of combustion where the flame radii are much smaller.

Figure 8 and 9 shows the variation of calculated flame thickness against equivalence ratio and CO_2. In general, flame thickness are larger for leaner mixtures. It also shows quadratic trend with equivalence ratio where it reaches its minimum point at φ = 0.8 where the fastest flame was observed. Fastest flame would have thinnest flame due to its highest reactivity. All flames across

equivalence ratio did not experience cellularity or buoyancy even though flame thickness fluctuate sharply with equivalence ratio. Flame thickness has a stabilizing properties by hindering cells formation. For an outwardly propagating spherical flame, this is due to curvature effect and baroclinicity [19]. Absence of cellularity shows that the thickness of all flames is sufficiently large to hinder cellularity formation. If the size of cells are in the order of flame thickness magnitude, cellularity could be caused mostly by diffusional-thermal instability. Larger cells formation on the other hand are caused by hydrodynamic and buoyancy driven instability [38]. Flames of leaner mixtures (φ = 0.7 and 0.8) also shows an approximately quadratic trend as CO_2 increases, while a linear trend was observed for richer mixture (φ =0.9). Flame thickness also influence the intensity of baroclinic torque that could arise from misalignment of pressure and density gradient. Baroclinic torque which arises from wrinkling flame surface could be enhanced by both flame thickness and density ratio [19].

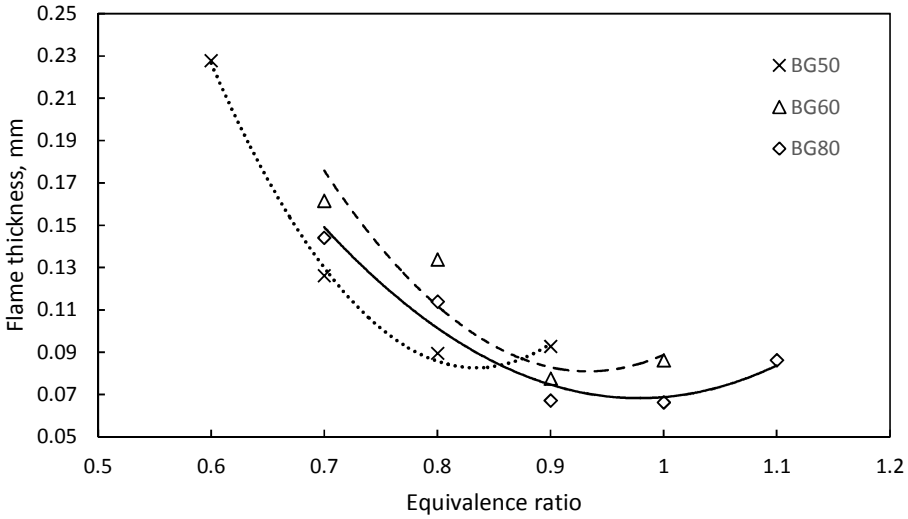

Fig. 8. Variation of flame thickness against equivalence ratio for each fuel mixture.

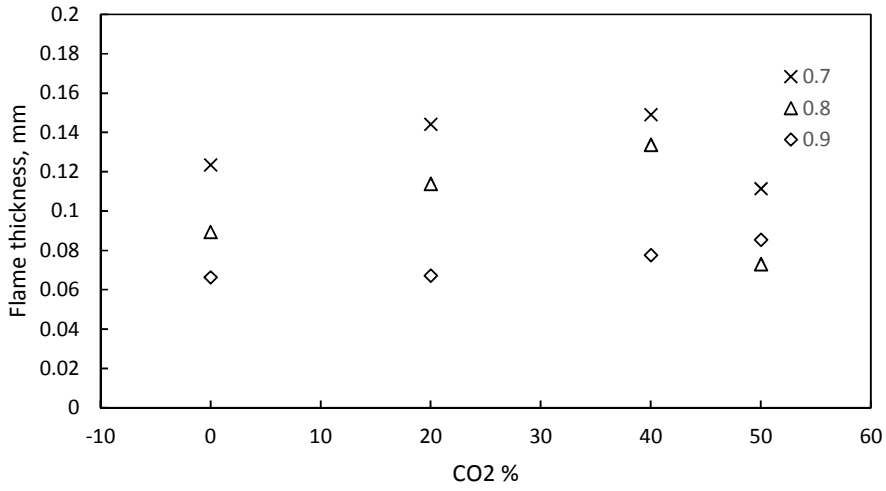

Fig. 9. Variation of flame thickness against CO_2 percentage for each fuel mixture. Explain this differing trend between 0.7, 0.8 and 0.9 flames.

Figure 10 shows the variation of density ratio against CO_2 percentage for each fuel mixture. Apparently CO_2 tend to reduce density ratio. The trend of density ratio seems to correspond to flame temperature (Figure 6) indicating that a decrease in flame temperature will lead to an equivalent decrease in density ratio suppressing hydrodynamic instability.

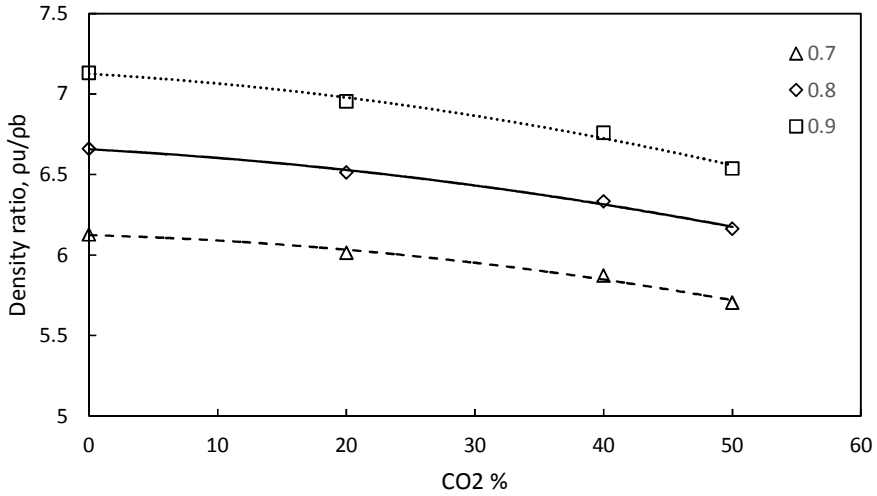

Fig. 10. Variation of density ratio against CO_2 percentage for each fuel mixture.

4. Conclusions

The effect of CO_2 on biogas combustion has been thoroughly investigated in this study. Apparently, there is a linear correlation between CO_2 percentage and biogas burning rate reduction. Reduction in burning rate could be linked to both chemical and physical effects of CO_2. Flammability also become narrower as CO_2 increases. Shift in lean limit was observed at highest CO_2 dilution due to formation of local equivalence ratio within the flame zone. Shift in peak burning rate to leaner side as CO_2 dilution increases is also more prominent compared to previous studies especially for BG50 due to perturbation of equilibrium by CO_2. Markstein length variation with equivalence ratio of all biogas mixtures shares a similar trend to pure CH_4 but with a higher value, indicating better flame stabilization due to suppression of thermal-diffusion instability. Calculated flame thickness and density ratio also suggest the suppression of hydrodynamic instability. Therefore there seem to be a trade-off between increase in stability and reduction in flame speed and burning rate as CO_2 content increases in biogas.

Acknowledgement
The authors would like to thank Ministry of Higher Education of Malaysia (MOHE) and Universiti Teknologi Malaysia for supporting this research activity under the Research Grant Scheme No. R.J130000.7824.4F749.

References

[1] Shafiee S., Topal E. When will fossil fuel reserves be diminished?. *Energy Policy* 37, (2009)::181-189.
[2] Schoen E.J. and Bagley D.M. Biogas Production and Feasibility of Energy Recovery Systems for Anaerobic Treatment of Wool-Scouring Effluent. *Resources, Conservation and Recycling* 62, (2012): 21-30.

[3] Sinaga N., Nasution, S.B., Mel, M. Process Optimization of Biogas Production from Palm Oil Mill Effluent: A Case Study of a Crude Palm Oil Factory in Muaro Jambi, Indonesia. *Journal of Advanced Research in Fluid Mechanics and Thermal Sciences* 49, (2018): 155-169.
[4] Fischer, M. and Jiang, X. An Investigation of the Chemical Kinetics of Biogas Combustion. *Fuel* 2015; 150:711-720.
[5] Chen, Z. Effects of radiation and compression on propagating spherical flames of methane/air mixtures near the lean flammability limit. *Combustion and flame,* 157(2010): 2267-2276.
[6] Chen Z. Effects of radiation absorption on spherical flames propagation and radiation-induced uncertainty in laminar flame speed measurement. *Proceeding of the combustion institute,* 36 (2017): 1129-1136.
[3] Xie, Y.L., Wang, J.H., Zhang, M., Gong, J., Jin, W., Huang, Z.H. Experimental and Numerical Study on Laminar Flame Characteristics of Methane Oxy-fuel Mixtures Highly Diluted with CO_2. *Energy and Fuel* 27, (2013): 6231-6237.
[4] Pizutti, L., Martins, C.A., and Lacava, P.T. Laminar Burning Velocity and Flammability Limits in Biogas: A Literature Review. *Renewable and Sustainable Energy Reviews* 62, (2016): 856-865.
[5] Bosschaart, K.J and de Goey L.P.H. The laminar burning velocity of flames propagating in mixtures of hydrocarbons and air measured with the heat flux method. *Combustion and Flame* 136, (2004): 261–269.
[6] Konnov, A.A., Dyakov, I.V, De Ruyck, J. Measurement of adiabatic burning velocity in ethane–oxygen–nitrogen and in ethane–oxygen–argon mixtures. *Exp. Therm. Fluid Sci*. 27, (2003): 379–384.
[7] Chao, B.H., Egolfopoulos, F.N., Law, C.K. Structure and propagation of premixed flame in nozzle-generated counterflow, *Combustion and Flame* 109, (1997): 620–638.
[8] Jackson, G.S., Sai, R., Plaia, J.M., Boggs, C.M., Kiger, K.T. Influence of H_2 on the response of lean premixed CH_4 flames to high strained flows. *Combustion and Flame* 132, (2003): 503–511.
[9] Taylor, S.C. (1991). Burning velocity and the effect of flame stretch. PhD Thesis; University of Leeds.
[10] Hassan M.I., Aung, K.T., Faeth, G.M. Measured and predicted properties of laminar premixed methane/air flames at various pressures. *Combustion and Flame* 115, (1998): 539–550.
[11] Gu, X.J., Haq, M.Z., Lawes, M., Woolley, R. Laminar burning velocity and Markstein lengths of methane–air mixtures. *Combustion and Flame* 121, (2000): 41–58.
[12] Rozenchan, G., Zhu, D.L., Law, C.K., Tse, S.D. Outward propagation, burning velocities, and chemical effects of methane flames up to 60 atm. *Proceedings of the Combustion Institute* 29, (2002): 1461–1469.
[13] Bradley, D., Hicks, R.A., Lawes, M., Sheppard, C.G.W., Woolley, R. The Measurement of Laminar Burning Velocities and Markstein Numbers for Iso-octane–Air and Iso-octane–nHeptane–Air Mixtures at Elevated Temperatures and Pressures in an Explosion Bomb. *Combustion and Flame* 115, (1998):126-144.
[14] Gillespie, L., Lawes, M., Sheppard, C.G.W., Woolley, R. Aspects of Laminar and Turbulent Burning Velocity Relevant to SI Engines. *Society of Automotive Engineers*, (2000): 2000-01-0192.
[15] Kwon, O.C., Rozenchan, G., and Law, C.K. Cellular Instabilities and Self-Acceleration of Outwardly Propagating Spherical Flames. *Proceedings of the Combustion Institute* 29, (2002): 1775–1783.
[16] Zhen, H.S., Leung, C.W., Cheung, C.S. Effects of hydrogen addition on the characteristics of a biogas diffusion flame. *International Journal of Hydrogen Energy* 38, (2013): 6874-81.
[17] Nonaka, H.O.B. and Pereira, F.M. Experimental and numerical study of CO_2 content effects on the laminar burning velocity of biogas. *Fuel* 182, (2016): 382–390.
[18] Moghaddam, E.A., Ahlgren, S., Hulteberg, C., Nordberg, Å. Energy balance and global warming potential of biogas-based fuels from a life cycle perspective. *Fuel Processing Technology* 132, (2015): 74–82.
[19] Zhen, H.S., Leung, C.W., Cheung, C.S., Huang, Z.H. Characterization of biogas-hydrogen premixed flames using Bunsen burner. *International Journal of Hydrogen Energy* 39, (2014): 13292-13299.
[20] Clarke, A. Calculation and consideration of the Lewis number for explosion studies. *Trans IChemE* 80, (2002): 135-140.
[21] Dinkelacker, F., Manickam, B., Muppala, S.P.R. Modelling and simulation of lean premixed turbulent methane/hydrogen/air flames with an effective Lewis number approach. *Combustion and Flame* 158, (2011): 1742-1749.
[22] Vanag, V.K. and Epstein, I.R. Cross-diffusion and pattern formation in reaction-diffusion systems. *Physical Chemistry Chemical Physics* 11, (2009): 897-912.
[23] Cardona, C. and Amell, A.A. Laminar burning velocity and interchangeability analysis of biogas/C_3H_3/H_2 with normal and oxygen-enriched air. *International Journal of Hydrogen Energy* 39, (2013): 7994-8001.
[24] Fischer, M. and Jiang X. An Investigation of the Chemical Kinetics of Biogas Combustion. *Fuel* 150, (2015): 711-720.
[25] Law, C.K., Jomaas, G., Bechtold, J.K. Cellular instabilities of expanding hydrogen/propane spherical flames at elevated pressures: theory and experiment. *Proceedings of the Combustion Institute* 30, (2005): 159-167.

[26] Tang, C., Huang, Z., Jin, C., He, J., Wang, J., Wang, X., et al. Laminar burning velocities and combustion characteristics of propane-hydrogen-air premixed flames. *International Journal of Hydrogen Energy* 33, (2008): 4906-14.
[27] Hinton, N. and Stone R. Laminar burning velocity measurements of methane and carbon dioxide mixtures (biogas) over wide ranging temperatures and pressures. *Fuel* 116, (2014): 743-750.
[28] Mameri, A. and Tabet, F. Numerical investigation of counter-flow diffusion flame of biogas–hydrogen blends: Effects of biogas composition, hydrogen enrichment and scalar dissipation rate on flame structure and emissions. *International Journal of Hydrogen Energy* 41, (2016): 2011–2022.
[29] Kelley, A.P. and Law, C.K. Nonlinear effects in the extraction of laminar flame speeds from expanding spherical flames. *Combustion and Flame* 156, (2009): 1844-1851.
[30] Konnov A.A. Detailed reaction mechanism for small hydrocarbon combustion, release 0.5; 2000. <http://homepages.vub.ac.be/akonnov/>.
[31] Smith G.P., Golden D.M., Frenklach M., Moriarty N.W., Goldenberg B.E.M., Bowman, Hanson R.K,, Song, S., [32] Gardiner, W.C., Jr, Lissianski, V.V., and Qin, Z. http://www.me.berkeley.edu/gri_mech/ .
[33] Han W. and Chen Z. Effects of Soret diffusion on spherical flame initiation and propagation. *International Journal of Heat and Mass Transfer* 82, (2015): 309–315.
[34] Suhaimi, M.S., Saat, A., Wahid, M.A., Sies, M.M. Flame Propagation and Burning Rates of Methane-Air Mixtures Using Schlieren Photography. *Jurnal Teknologi* 78, (2016): 21-27.
[35] Law C.K. (2006). *Combustion Physics*, Cambridge University Press.